nature climate change

SUPPLEMENTARY INFORMATION

DOI: 10.1038/NCLIMATE2808

Linear sea-level response to abrupt ocean warming of major West Antarctic ice basin

M. Mengel, J. Feldmann and A. Levermann

Potsdam Institute for Climate Impact Research, Potsdam, Germany.

Institute of Physics, Potsdam University, Potsdam, Germany.

This supplement provides additional information on the parameters used for the regional and whole-continent ensemble, figures on equilibrium and retreated ice-sheet states and a description of the pressure adaption for basal melting. The parameters that are varied within the PISM ensemble to cover the main uncertainties in ice-sheet flow are listed in Tab. S1 for the regional simulations and Tab. S2 for the whole-continent simulations. In the PISM model the ice velocities are calculated by superposition of two shallow stress balance approximations: the shallow ice approximation (SIA) that is dominant in grounded regions and accounts for the shear deformation of the ice, see Winkelmann et al. [2011] equation (7), and the plug-flow type shallow shelf approximation (SSA) that dominates the velocity field in ice shelves and ice streams, see Winkelmann et al. [2011] equations (8) and (9). The pore water fraction (pw) determines to which part the thermodynamically-derived basal water thickness is translated to basal water pressure, which in turn influences the effective pressure and basal yield stress, see Bueler and Brown [2009] equation (20) where a fixed pore water fraction of 0.95 is used.

Thickness calving removes all floating ice along the ice front that is thinner than the provided threshold value in the tables. For the eigencalving mechanism see Levermann et al. [2012].

Fig. S1 shows the regional equilibrium state and the response of the ice thickness, calving front and grounding line to strong melt forcing. Fig. S2 shows the same for the whole-continent simulations. Equilibrium grounding line and calving front positions are free to evolve in the PISM model and generally compare well to the observed state (panels a). Fig. S3 shows the difference between two states that are representative for the (1) linear response valid for stronger forcings and the (2) weaker response under relatively weak forcing.

As we apply basal melting from ocean model simulations that use a fixed geometry for the ice-shelf, there is a need to correct the basal melt rates to the time-varying ice-shelf thickness of the PISM simulations. We present a parametrization for the pressure-adaption of basal melt in the section below.

Table S1: Parameter combinations for regional simulations that yielded stable grounding lines not significantly deviating from the observed state [Fretwell et al., 2013]. SIA, SSA and PW refer to shallow ice approximation enhancement factor, shallow shelf approximation enhancement factor and basal pore water fraction, respectively. For details on the pore water fraction in PISM see (Martin et al. 2011). thk and eigenK refer to the thickness calving threshold and the eigencalving parameter K (Levermann et al. 2012). Forcing experiments were branched from each of the listed equilibrium states.

experiment id	ice flow and basal friction	calving
reg1	sia 2.0 ssa 0.8 pw 0.91	thk 200m eigenK 1e16
reg2	sia 4.5 ssa 0.8 pw 0.95	thk 200m eigenK 1e16

Table S2: Parameter combinations for whole-Antarctica equilibrium simulations that yielded stable grounding lines around all Antarctica; SIA, SSA and PW refer to shallow ice approximation enhancement factor, shallow shelf approximation enhancement factor and basal pore water fraction, respectively. thk and eigenK refer to the thickness calving threshold and the eigencalving parameter K. Forcing experiments were branched from each of the listed equilibrium states. See Tab S1 for references.

experiment id	ice flow and basal friction	calving
ant1	sia 2.0 ssa 0.5 pw 0.90	thk 200m eigenK 1e15
ant2	sia 2.0 ssa 0.6 pw 0.92	thk 170m eigenK 1e17
ant3	sia 2.0 ssa 0.8 pw 0.94	thk 170m eigenK 1e15
ant4	sia 2.0 ssa 0.8 pw 0.90	thk 170m eigenK 1e17
ant5	sia 4.5 ssa 0.5 pw 0.90	thk 200m eigenK 1e15

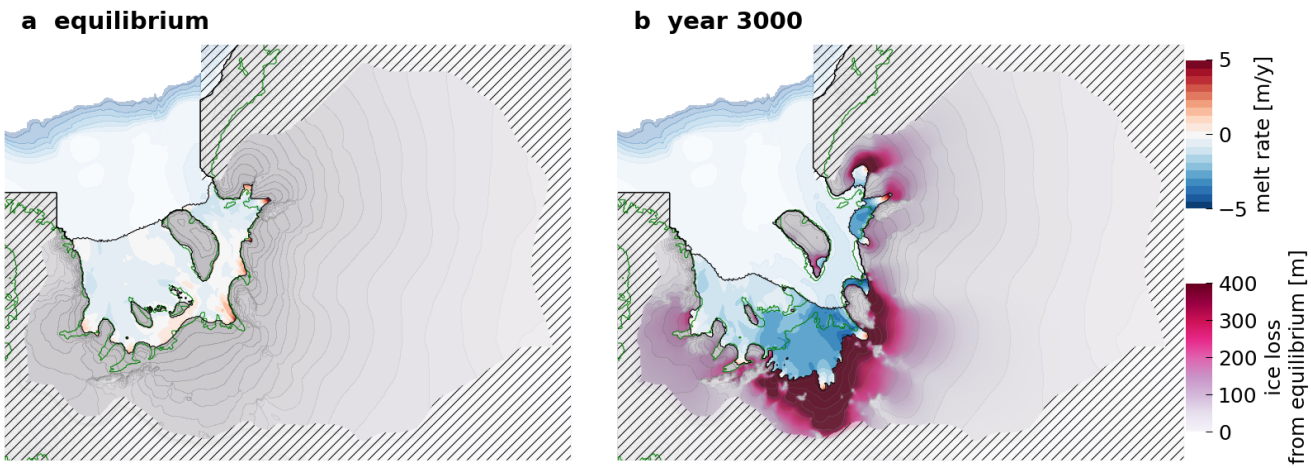

Figure S1: Regional equilibrium state (left panel) for parameter set reg2 and the response after 1000 yr to the strongest 2190-2200 melt forcing for 320 yr and equilibrium conditions applied afterwards (right panel). Ice thinning is indicated by red shading. Contours show surface elevation, green line the observed grounding line [Fretwell et al., 2013] and black line the modeled grounding line and calving front. Equilibrium melt rates may be compared to Moholdt et al. [2014].

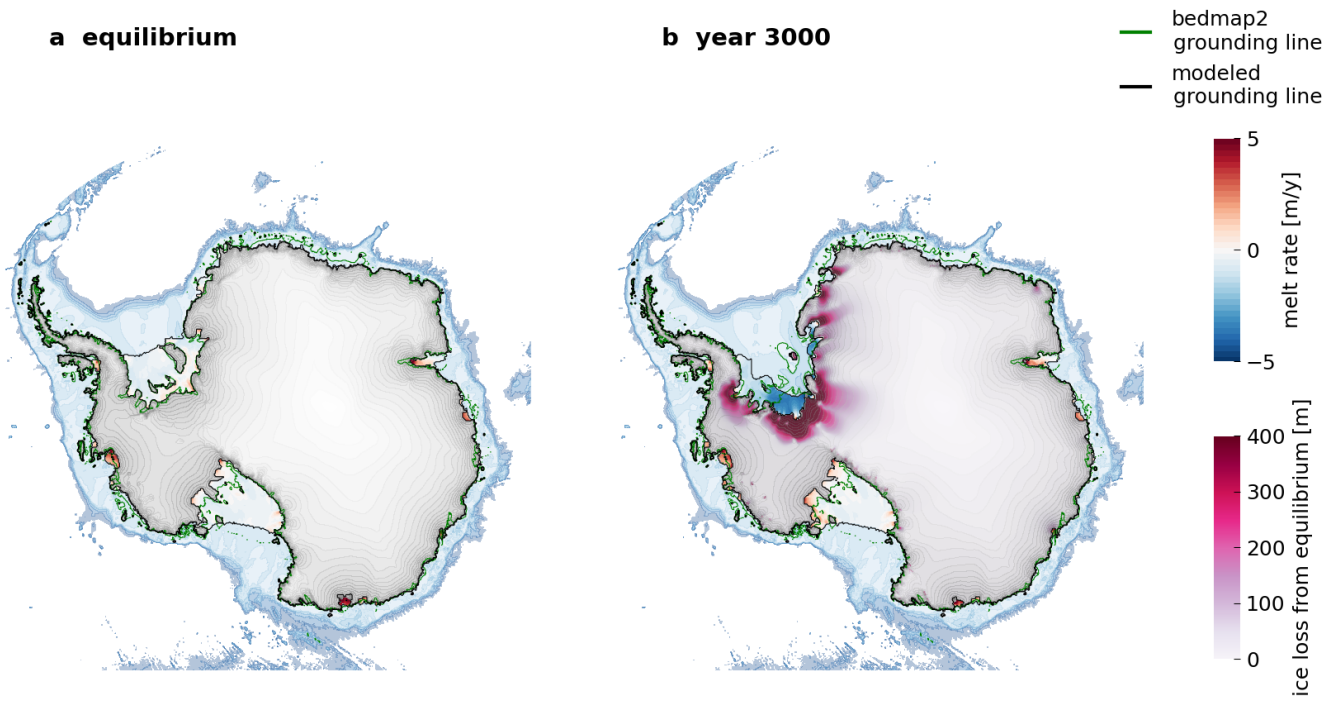

Figure S2: Whole-Antarctica equilibrium state (left panel) for parameter set ant4 (left panel) and the response after 1000 yr to the strongest 2190-2200 melt forcing for 320 yr and equilibrium conditions applied afterwards (right panel). Ice thinning is indicated by red shading. Contours show surface elevation, green line the observed grounding line [Fretwell et al., 2013] and black line the modeled grounding line and calving front.

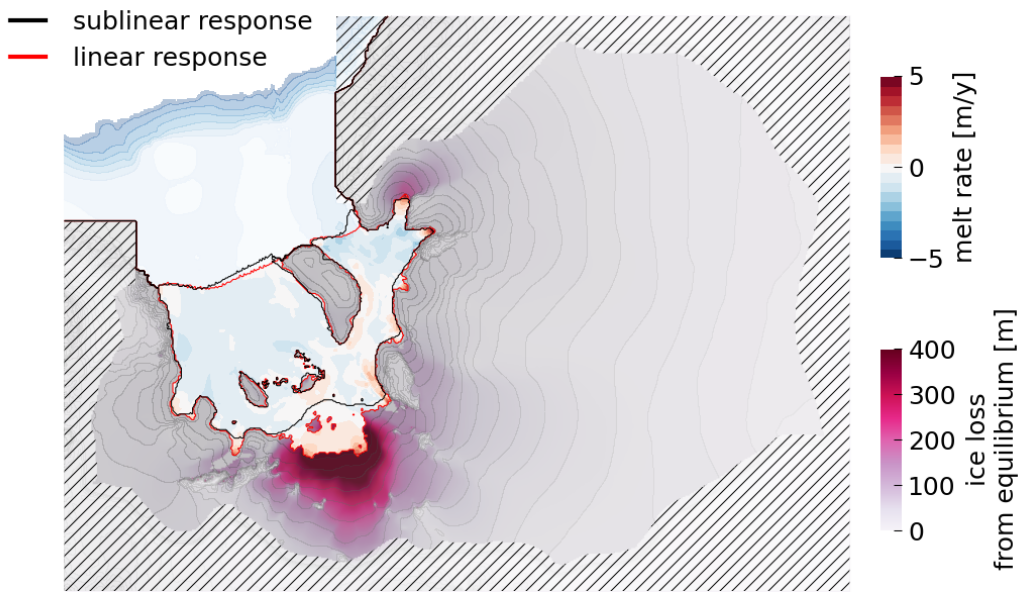

Figure S3: Difference between two representative states from the linear regime (experiment reg2 320y forcing with 2140-2150 pulse; red cross in Fig. 4) and the weaker-response regime (experiment reg1 160y forcing with 2100-2110 pulse; black cross in Fig. 4). The linear sensitivity over the wide range of melt forcing is linked to the ungrounding of the ice plains as part of the Institute and Möller ice streams. The ungrounding is indicated by the retreated grounding line (red) as compared to the more stable grounding line (black). The difference in grounded ice thickness loss is shown as red shading over grounded ice. Shading over the shelf indicates the basal melting for the retreated state.

Calving

We apply a physical stress boundary condition at the calving front to close the equation for the shallow shelf approximation [Winkelmann et al., 2011]. The boundary condition features geographically confined ice shelves. Calving is calculated through the Eigencalving parametrization [Levermann et al., 2012] and from an ice thickness condition [Albrecht et al., 2011]. The set of parametrizations has been shown to yield realistic calving front positions [Martin et al., 2011].

Pressure melt adaption

We apply a parametrization that adjusts basal melting fields from ocean models coupled to static ice shelves to the time-evolving ice-shelf geometry in ice models. It accounts for the pressure dependence of the seawater freezing point and translates it to a melt-rate dependence on ice-shelf thickness.

At present most large-scale ocean models are based on temporally fixed grids that cannot adapt to evolving ice-shelf geometries. The existing coupled ice-ocean models apply an ice-sheet model with fixed ice-shelf geometry [Hellmer, 2004, Losch, 2008, Timmermann and Hellmer, 2013, Dutrieux et al., 2014]. The forcing of ice-sheet models with melt rates (uni-directional coupling) excludes the feedbacks between ice and ocean, for example the steepness of the ice-shelf cavity influencing the sub-shelf ocean circulation [Hellmer and Olbers, 1989, Jenkins, 1991, Grosfeld et al., 1997, Beckmann et al., 1999, Little et al., 2009] or the effect of ice-shelf meltwater on the sea ice distribution [Bintanja et al., 2013]. One important feedback can however be easily included in uni-directionally coupled runs, that is the pressure dependence of heat availability for basal melting. The presented parametrization adapts the basal melt rates to changing pressure, based on the equilibrium boundary layer approach [Hellmer et al., 1998, Holland and Jenkins, 1999].

At the underside of an ice-shelf heat and salinity fluxes from the ocean balance the latent heat sink and the freshwater input from melting in the boundary layer as well as the heat loss into the ice-shelf. Temperature and salinity from the well-mixed ocean mainly determine the basal melt rate

in this system in conjunction with the local pressure. These ocean fields are however not always available for the coupling to ice-sheet models. Furthermore, picking ocean and salinity values at right distance from the ice-shelf can be difficult as they need to represent well-mixed conditions and the local water mass imprint at the same time. This is especially difficult if the ocean model was coupled to a static ice-shelf model during runtime (as in the FESOM model from which we apply the output in this study), because the mixing with melt water affects the salinity and temperature outside the boundary layer.

Alternatively driving ice-sheet models directly with the ocean-model-derived melt rates does not reflect the pressure dependence of the melting. Our parametrization helps to reduce this problem. We show that the melt rate dependence on pressure can well be approximated as a function of the melt rate alone. We provide an exponential fit of the function that serves as a simple pressure-dependence parameterization. The fitted univariate function makes pressure adaption of melt rates possible without the explicit knowledge of ocean salinity and temperature.

For the derivation of the melting rate an equilibrium approach for the boundary layer between ice and ocean [Hellmer et al., 1998, Holland and Jenkins, 1999] has been widely adopted [Timmermann et al., 2002, Holland et al., 2008, Timmermann and Hellmer, 2013, Dutrieux et al., 2014]. In equilibrium, the heat and salinity flux from the ocean balances the salinity and temperature changes due to melting and refreezing in the boundary layer at the ice-ocean interface as well as the heat loss into the ice. The corresponding physical system can be described by three physical constraints leading to three coupled equations. The three constraints are: the interface between ocean and ice-shelf must be at the freezing point and both heat and salt must be conserved at the interface during any phase changes. This system can be solved if a linearized freezing point equation is adopted. Several solutions have been proposed and their main difference lies in the treatment of the heat flux through the ice-shelf and the parametrization of turbulent fluxes between the boundary layer and the ocean, see the discussion in Holland and Jenkins [1999]. Melting generates a nonlinear temperature profile in the ice column. Here we adopt the solution of Wexler [1960] for melt rates

larger than zero that incorporates vertical and neglects horizontal advection of heat, see also Eq. 13 in Hellmer et al. [1998] and Eq. 22 in Holland and Jenkins [1999]. The approach is not valid in a refreezing situation. For this case we treat the ice-shelf as a perfect insulator with a temperature gradient of zero in the ice, following Eq. 31 in Holland and Jenkins [1999]. We assume constant exchange velocities for temperature and salinity with values taken from Hellmer et al. [1998].
Under these assumptions, the melting/refreezing rate m is primarily a function of ocean salinity, ocean temperature and pressure.

$$m = m(T_{\text{ocean}}, S_{\text{ocean}}, \text{pressure}, ...) \tag{1}$$

The pressure enters through the linearized melting point equation and is a linear function of depth z when water density is assumed constant:

$$T_{\text{melt}} = aS_{\text{bound}} + b + cz \tag{2}$$

For small changes in z, the z-dependence of the melting can be approximated as:

$$m(z) = m0 + \left.\frac{dm}{dz}\right|_{z_0} \cdot (z - z_0) \tag{3}$$

Where $m(z)$ is the desired melt rate to interact with the ice-sheet model and $m0$ is the melt rate available from the ocean model. The derivative is in general a function of the system's variables. However, as we show in Fig. S4, these dependencies are largely incorporated in the dependence on the meltrate itself over a wide range of depths, ocean temperatures and ocean salinities, it is thus justified to approximate it as a univariate function of m, which is the approach that we follow here:

$$\left.\frac{dm}{dz}\right|_{z_0} = f(m) \tag{4}$$

We can therefore parametrize the depth-dependence of melting as

$$m(z) = m_0 + f(m) \cdot (z - z_0) \tag{5}$$

We choose to fit f(m) with an exponential function, so that

$$f(m) = \left.\frac{dm}{dz}\right|_{z_0} = 0.030 - 0.024 \cdot e^{-0.026 \cdot m} \tag{6}$$

with melting in units of m/year and positive values representing ice mass loss. The fit is shown as a red line in Fig. S4. This parametrization relies only on an input meltrate m_0, for example from an ocean model, and the reference thickness z_0 at which m_0 has been calculated. It is consistent with the equilibrium boundary layer approach and does not rely on the ocean salinity and temperature fields directly.

In Fig. S5 we show the difference between the melt rate derived from solving the 3-equation system and from the parametrization for a shelf thickness change of $\pm$100m and $\pm$200m, starting from original ice-shelf thickness z_0 between 500m and 2000m (Fig. S5 , x-axes). The temperature and salinity tuples are representative for the different water masses around Antarctica. For most cases the error is smaller than 1 percent. The error is generally higher when melt rates are reduced, that is when the ice-shelf thins (Fig. S5 , lines with squares). For high melt rates the absolute error (Fig. S5 , left panels) is higher, but the relative error very small. Relative errors (Fig. S5 , right panels) are high for very small melting or refreezing close to zero, particularly at the transition between melting and refreezing (red line with squares). Other errors are however probably dominant for very small melt or refreezing. The parameterization and the full solution do not diverge even for larger deviations from the original geometry.

The pressure-adaption parametrization approximates the pressure dependence of basal melting that originates from the freezing point dependence on pressure. Open-ocean waters that carry heat and salt typically arrive at greater depth and then rise towards the calving front while they entrain cold

and fresh meltwater. This generally yields a typical pattern with higher temperatures and salinities at the grounding line that decrease towards the calving front. We do not attempt to cover the melt variation [Jenkins and Doake, 1991, Rignot, 2002] due to this temperature and salinity pattern in our parametrization. The parametrization is designed for input fields from ocean circulation models that explicitly model the circulation in the shelf cavity, so that the variance of temperature and salinity fields is assumed to be covered in the ocean-model data. For parameterizations that cover the indirect depth dependence of melting through the depth-dependent pattern of temperature and salinity, we refer to [Hellmer and Olbers, 1989, Jenkins, 1991, Grosfeld et al., 1997, Beckmann et al., 1999, Beckmann and Goosse, 2003, Little et al., 2009].

The pressure-adaption introduces a negative feedback for ice-shelf melting distant from the grounding line since shallower shelves yield reduced melting. This may overestimate the stability of ice-shelves as other potentially positive feedbacks with the ocean circulation are not covered. However, near the grounding line the parameterization yields a positive feedback on a downsloping bedrock. When the grounding line retreats into deeper basins the melting is increased under higher pressure. This is particularly important for the forcing during a marine ice-sheet instability [Schoof, 2007].

Heat and salt is not conserved in the parametrization. This is a general problem of uni-directional coupling as heat and salinity changes cannot be passed back to the ocean model. While the pressure parameterization clearly cannot substitute fully coupled simulations, it improves the applicability of static-geometry ocean field data to ice-sheet models with dynamic ice-shelves and covers the feedback between ice-shelf geometry and ocean circulation that is accessible without a full ice-ocean coupling.

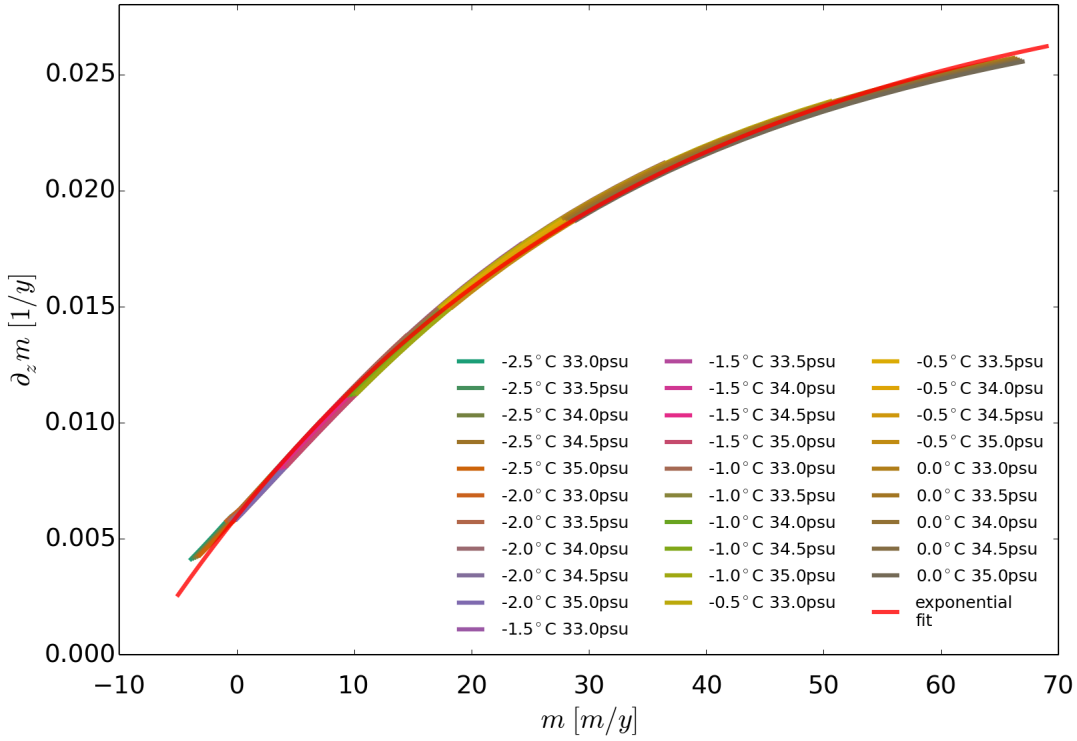

Figure S4: Dependence on the basal melt rate of dm/dz = f(m) calculated from the 3-equation system for different salinities and temperatures (short coloured lines) and fitted with an exponential function (red line). f(m) is largely independent of salinity and temperature and can therefore be well approximated by the univariate exponential function. The fit can thus serve as a simple parameterization for the pressure-dependence of basal melting which allows to adapt the basal melt rate to changing pressure without the knowledge of the salinity and temperature field. Coefficients of the fit as in equation (6).

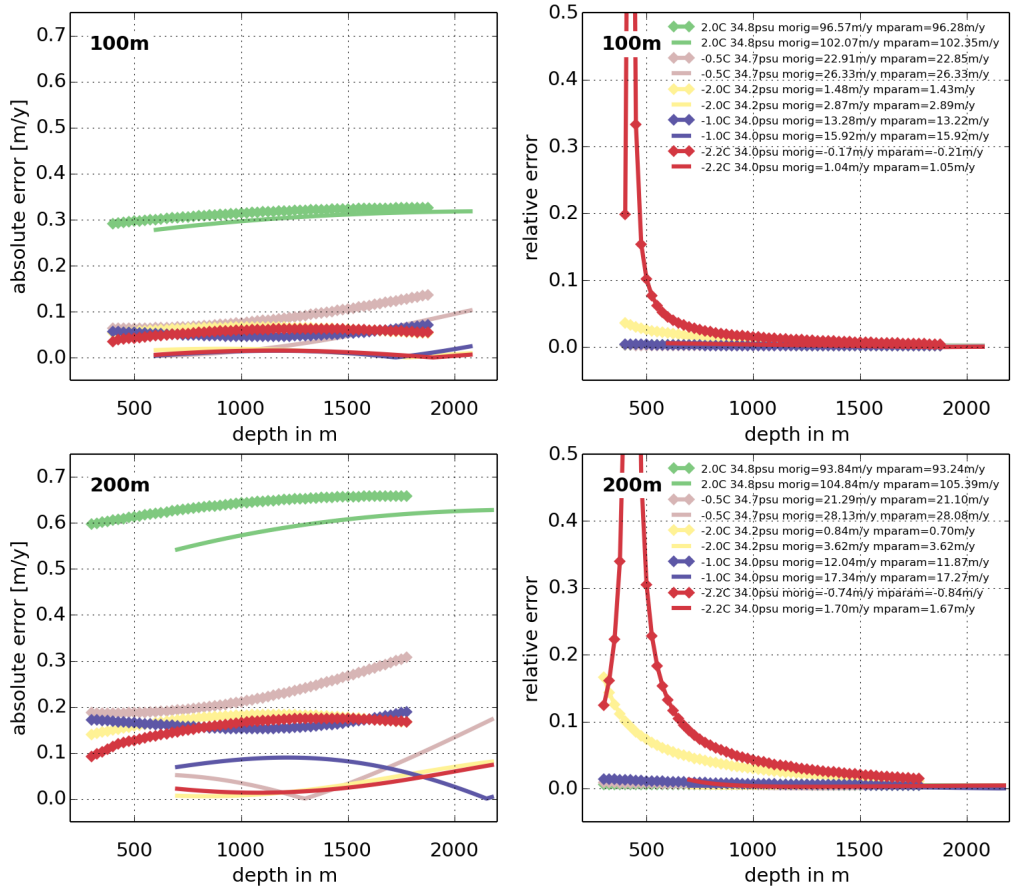

Figure S5: Absolute (left panels) and relative error (right panels) between full basal-melt rate according to the 3-equation-calculation and the approximation used here for different temperature and salinity tuples that are representative for Antarctic water masses. Ice thickness deviates by +- 100m (upper panels) and +- 200m (lower panels) from the original thickness. The unbound relative errors (red lines with squares, right panels) are due to the transition from melting to refreezing, so the denominator passes zero. Legend entries show water mass properties and the tuple of fully-derived melt rate (morig) and from the parametrization (mparam) for the depth where the error is maximum.

References

T. Albrecht, M. Martin, M. Haseloff, R. Winkelmann, and A. Levermann. Parameterization for subgrid-scale motion of ice-shelf calving fronts. *The Cryosphere*, 5(1):35–44, January 2011. ISSN 1994-0424. doi: 10.5194/tc-5-35-2011. URL http://www.the-cryosphere.net/5/35/2011/tc-5-35-2011.html.

A Beckmann and H Goosse. A parameterization of ice shelfocean interaction for climate models. *Ocean Modelling*, 5(2):157–170, January 2003. ISSN 14635003. doi: 10.1016/S1463-5003(02)00019-7. URL http://linkinghub.elsevier.com/retrieve/pii/S1463500302000197.

A Beckmann, H. H. Hellmer, and Ralph Timmermann. A numerical model of the Weddell Sea: Large-scale circulation and water mass distribution. *Journal of Geophysical Research*, 104(C10):23375, 1999. ISSN 0148-0227. doi: 10.1029/1999JC900194. URL http://onlinelibrary.wiley.com/doi/10.1029/1999JC900194/abstract.

R. Bintanja, G. J. van Oldenborgh, S. S. Drijfhout, B. Wouters, and C. A. Katsman. Important role for ocean warming and increased ice-shelf melt in Antarctic sea-ice expansion. *Nature Geoscience*, 6(5):376–379, March 2013. ISSN 1752-0894, 1752-0908. doi: 10.1038/ngeo1767. URL http://www.nature.com/doifinder/10.1038/ngeo1767.

Ed Bueler and Jed Brown. Shallow shelf approximation as a sliding law in a thermomechanically coupled ice sheet model. *Journal of Geophysical Research*, 114(F3), July 2009. ISSN 0148-0227. doi: 10.1029/2008JF001179. URL http://onlinelibrary.wiley.com/doi/10.1029/2008JF001179/abstract.

P. Dutrieux, J. De Rydt, A. Jenkins, P. R. Holland, H. K. Ha, S. H. Lee, E. J. Steig, Q. Ding, E. P. Abrahamsen, and M. Schroder. Strong Sensitivity of Pine Island Ice-Shelf Melting to Climatic Variability. *Science*, 343(6167):174–178, January 2014. ISSN 0036-8075, 1095-9203. doi:

10.1126/science.1244341. URL http://www.sciencemag.org/cgi/doi/10.1126/science.1244341.

P. Fretwell, H. D. Pritchard, D. G. Vaughan, J. L. Bamber, N. E. Barrand, R. Bell, C. Bianchi, R. G. Bingham, D. D. Blankenship, G. Casassa, G. Catania, D. Callens, H. Conway, A. J. Cook, H. F. J. Corr, D. Damaske, V. Damm, F. Ferraccioli, R. Forsberg, S. Fujita, Y. Gim, P. Gogineni, J. A. Griggs, R. C. A. Hindmarsh, P. Holmlund, J. W. Holt, R. W. Jacobel, A. Jenkins, W. Jokat, T. Jordan, E. C. King, J. Kohler, W. Krabill, M. Riger-Kusk, K. A. Langley, G. Leitchenkov, C. Leuschen, B. P. Luyendyk, K. Matsuoka, J. Mouginot, F. O. Nitsche, Y. Nogi, O. A. Nost, S. V. Popov, E. Rignot, D. M. Rippin, A. Rivera, J. Roberts, N. Ross, M. J. Siegert, A. M. Smith, D. Steinhage, M. Studinger, B. Sun, B. K. Tinto, B. C. Welch, D. Wilson, D. A. Young, C. Xiangbin, and A. Zirizzotti. Bedmap2: improved ice bed, surface and thickness datasets for Antarctica. *The Cryosphere*, 7(1):375–393, February 2013. ISSN 1994-0424. doi: 10.5194/tc-7-375-2013. URL http://www.the-cryosphere.net/7/375/2013/.

K. Grosfeld, R. Gerdes, and J. Determann. Thermohaline circulation and interaction between ice shelf cavities and the adjacent open ocean. *Journal of Geophysical Research*, 102(C7): 15595, 1997. ISSN 0148-0227. doi: 10.1029/97JC00891. URL http://onlinelibrary.wiley.com/doi/10.1029/97JC00891/abstract.

H. H. Hellmer. Impact of Antarctic ice shelf basal melting on sea ice and deep ocean properties. *Geophysical Research Letters*, 31(10), 2004. ISSN 0094-8276. doi: 10.1029/2004GL019506. URL http://onlinelibrary.wiley.com/doi/10.1029/2004GL019506/abstract.

H. H. Hellmer and D.J. Olbers. A two-dimensional model for the thermohaline circulation under an ice shelf. *Antarctic Science*, 1(04), December 1989. ISSN 0954-1020, 1365-2079. doi: 10.1017/S0954102089000490. URL http://journals.cambridge.

org/action/displayAbstract?fromPage=online&aid=223291&fileId=S0954102089000490.

H. H. Hellmer, Stanley S. Jacobs, and Adrian Jenkins. Oceanic erosion of a floating Antarctic glacier in the Amundsen Sea. In Stanley S. Jacobs and Ray F. Weiss, editors, *Antarctic Research Series*, volume 75, pages 83–99. American Geophysical Union, Washington, D. C., 1998. ISBN 0-87590-910-8. URL http://onlinelibrary.wiley.com/doi/10.1029/AR075p0083/summary.

David M. Holland and Adrian Jenkins. Modeling Thermodynamic IceOcean Interactions at the Base of an Ice Shelf. *Journal of Physical Oceanography*, 29(8):1787–1800, August 1999. ISSN 0022-3670, 1520-0485. doi: 10.1175/1520-0485(1999)029⟨1787:MTIOIA⟩2.0.CO;2.

Paul R. Holland, Adrian Jenkins, and David M. Holland. The Response of Ice Shelf Basal Melting to Variations in Ocean Temperature. *Journal of Climate*, 21(11):2558–2572, June 2008. ISSN 0894-8755, 1520-0442. doi: 10.1175/2007JCLI1909.1. URL http://journals.ametsoc.org/doi/abs/10.1175/2007JCLI1909.1.

A. Jenkins. A one-dimensional model of ice shelf-ocean interaction. *Journal of Geophysical Research*, 96(C11):20671, 1991. ISSN 0148-0227. doi: 10.1029/91JC01842. URL http://onlinelibrary.wiley.com/doi/10.1029/91JC01842/abstract.

A. Jenkins and C. S. M. Doake. Ice-ocean interaction on Ronne Ice Shelf, Antarctica. *Journal of Geophysical Research*, 96(C1):791, 1991. ISSN 0148-0227. doi: 10.1029/90JC01952. URL http://onlinelibrary.wiley.com/doi/10.1029/90JC01952/abstract.

A. Levermann, T. Albrecht, R. Winkelmann, M. A. Martin, M. Haseloff, and I. Joughin. Kinematic first-order calving law implies potential for abrupt ice-shelf retreat. *The Cryosphere*, 6(2):273–286, March 2012. ISSN 1994-0424. doi: 10.5194/tc-6-273-2012. URL http://www.the-cryosphere.net/6/273/2012/.

Christopher M. Little, Anand Gnanadesikan, and Michael Oppenheimer. How ice shelf morphology controls basal melting. *Journal of Geophysical Research: Oceans*, 114(C12):C12007, December 2009. ISSN 2156-2202. doi: 10.1029/2008JC005197. URL http://onlinelibrary.wiley.com/doi/10.1029/2008JC005197/abstract.

M. Losch. Modeling ice shelf cavities in a z-coordinate ocean general circulation model. *Journal of Geophysical Research*, 113(C8), August 2008. ISSN 0148-0227. doi: 10.1029/2007JC004368. URL http://doi.wiley.com/10.1029/2007JC004368.

M. A. Martin, R. Winkelmann, M. Haseloff, T. Albrecht, E. Bueler, C. Khroulev, and A. Levermann. The Potsdam Parallel Ice Sheet Model (PISM-PIK) Part 2: Dynamic equilibrium simulation of the Antarctic ice sheet. *The Cryosphere*, 5(3):727–740, September 2011. ISSN 1994-0424. doi: 10.5194/tc-5-727-2011. URL http://www.the-cryosphere.net/5/727/2011/.

Geir Moholdt, Laurie Padman, and Helen Amanda Fricker. Basal mass budget of Ross and Filchner-Ronne ice shelves, Antarctica, derived from Lagrangian analysis of ICESat altimetry. *Journal of Geophysical Research: Earth Surface*, page 2014JF003171, November 2014. ISSN 2169-9011. doi: 10.1002/2014JF003171. URL http://onlinelibrary.wiley.com/doi/10.1002/2014JF003171/abstract.

E. Rignot. Rapid Bottom Melting Widespread near Antarctic Ice Sheet Grounding Lines. *Science*, 296(5575):2020–2023, June 2002. ISSN 00368075, 10959203. doi: 10.1126/science.1070942. URL http://www.sciencemag.org/cgi/doi/10.1126/science.1070942.

Christian Schoof. Ice sheet grounding line dynamics: Steady states, stability, and hysteresis. *Journal of Geophysical Research*, 112(F3), July 2007. ISSN 0148-0227. doi: 10.1029/2006JF000664. URL http://doi.wiley.com/10.1029/2006JF000664.

R. Timmermann and H. H. Hellmer. Southern Ocean warming and increased ice shelf basal melting in the twenty-first and twenty-second centuries based on coupled ice-ocean finite-element modelling. *Ocean Dynamics*, 63(9-10):1011–1026, October 2013. ISSN 1616-7341, 1616-7228. doi: 10.1007/s10236-013-0642-0. URL http://link.springer.com/10.1007/s10236-013-0642-0.

R. Timmermann, A. Beckmann, and H. H. Hellmer. Simulations of ice-ocean dynamics in the Weddell Sea 1. Model configuration and validation. *Journal of Geophysical Research: Oceans*, 107(C3):10–1, March 2002. ISSN 2156-2202. doi: 10.1029/2000JC000741. URL http://onlinelibrary.wiley.com/doi/10.1029/2000JC000741/abstract.

H. Wexler. Heating and melting of floating ice shelves. *Journal of Glaciology*, 3:626–645, March 1960. ISSN 0022-1430. URL http://adsabs.harvard.edu/abs/1960JGlac...3..626W.

R. Winkelmann, M. A. Martin, M. Haseloff, T. Albrecht, E. Bueler, C. Khroulev, and A. Levermann. The Potsdam Parallel Ice Sheet Model (PISM-PIK) Part 1: Model description. *The Cryosphere*, 5(3):715–726, September 2011. ISSN 1994-0424. doi: 10.5194/tc-5-715-2011. URL http://www.the-cryosphere.net/5/715/2011/.